UNIVERSITÀ DI PARMA
ARCHIVIO DELLA RICERCA

University of Parma Research Repository

Hybrid polyelectrolyte/Fe3O4 nanocapsules for hyperthermia applications

Publisher copyright

note finali coverpage

(Article begins on next page)

03 July 2024

Hybrid polyelectrolyte/Fe3O4 nanocapsules for hyperthermia applications

Luigi Cristofolini[a]*, Krzysztof Szczepanowicz[b]*†, Davide Orsi[a], Tiziano Rimoldi[a], Franca Albertini[c], Piotr Warszynski[b]

[a] *Dipartimento di Fisica e Scienze della Terra- Parma University, Parma, Italy*

[b] *J. Haber Institute of Catalysis and Surface Chemistry PAS, Krakow, Poland*

[c] *Istituto IMEM-CNR, Parma, Italy*

Keywords: nanocapsules, hyperthermia, magnetic nanoparticles, biomedical application, drug delivery

Abstract

We validate here the applicability to hyperthermia treatment of magnetic nanocapsules with a polyelectrolyte shell around a nanodroplet liquid core prepared by the sequential Layer-by-Layer adsorption of polyelectrolytes and magnetic nanoparticles, around a nanodroplet liquid core. Biocompatible polyelectrolytes are used: Poly L-lysine as the polycation and Poly Glutamic acid as the polyanion.

The hyperthermia effect was demonstrated by applying a radio frequency (rf) magnetic field with maximum fields H up to 0.025 T and frequencies up to 430 kHz; we find sizeable heating effects, with heating rate up to 0.46°C/min. We also find effects of irradiation on capsules morphology that indicate their disruption, thus suggesting their potential use as drug nanocarriers. Therefore, these magnetically responsive nanocapsules could be a promising platform for multifunctional biomedical applications such as the controlled release of pharmaceuticals in combination with hyperthermia treatment.

Introduction

Magnetic nanoparticles have several applications in the biomedical field, exploiting their ability to be controlled at distance by external magnetic fields [1]. An important application is the hyperthermia cancer treatment: magnetic nanoparticles, irradiated with radio frequency magnetic fields, can induce localized heating into targeted cancer tissues, promoting cell death. Depending on the extent of local heat production, the temperature increase might have several effects on the cell [2]: (1) heating in the

range 41–46 ℃ induces cell apoptosis triggered by a controlled alteration of structural and enzymatic functions of cell proteins; (2) heating above 46–48 ℃ (usually up to 56 ℃) causes direct necrosis and coagulation. Furthermore, in the former case, moderate temperature increase enhances cells sensitivity to other treatments provided e.g. by radiation therapy or by chemotherapy. Moreover, tumor tissues possess a disorganized and compact vascular structure, their ability to dissipate heat is hindered; therefore, hyperthermia causes a stronger response in tumor tissues than in healthy tissues [3].

Microencapsulation of drugs is an effective way to produce versatile multifunctional carriers for drug delivery [4, 5]. Magnetic microcapsules offer the advantage of addressability and controlled release by externally applied magnetic fields of suitable geometry. Among others, polyelectrolyte nanocapsules prepared by the layer-by-layer (LbL) technique are considered to be particularly effective [6-8] for they biocompatibility, the relatively simple preparation protocols, the wide range of easy functionalization opportunities for tumor targeting and controlled opening. The polyelectrolyte multilayers are grown onto cores and the; growth steps can be followed in great detail [9]; inorganic, polymeric or hydrogel micro- and nanoparticles have been ~~considered~~ investigated ([10] and references therein). The use of emulsion nanodroplets as cores for encapsulation by the LbL adsorption [11-21] makes relatively easy to enclose active components inside the nanosized containers. Polyelectrolyte nanocapsules can be functionalized by magnetic nanoparticles, and then, they can be guided with magnetic field gradient to the desired tissue ~~of the organism~~ [22-24], to deliver biologically active material with an optimum therapeutic concentration of the pharmaceuticals. Moreover, exploiting the so-called "enhanced permeability and retention" (EPR) effect [25], magnetic nanocapsules may be promising tool for cancer treatment.

Furthermore, magnetic nanoparticles find use as contrast agents for magnetic resonance imaging (MRI), tissue repairing, cell tracking and bioseparation [26-30]. Of particular interest is the combined exploitation of different functionalities, allowing ~~simultaneous~~ the treatment and simultaneously the measurement of ~~the~~ its efficacy. ~~of the treatment.~~ This is called theranostics— the fusion of therapeutic functionality (e.g. drug carriers) and diagnostics (e.g. MRI imaging). Progress in theranostics is expected to pave the way towards the development of "individualized" medicine [31].

Common constituents used to impart magnetic properties are nanoparticles of iron, nickel, cobalt or their oxides. However, magnetic nanoparticles for biomedical application, besides chemical stability, should be non-toxic and biocompatible, with no negative impact at any level on cells, tissues and the

whole body. This limits the choice of viable compounds. Iron oxides, such as magnetite (Fe_3O_4) and maghemite ($\gamma\text{-}Fe_2O_3$), are superior to other metal oxide nanoparticles for their biocompatibility and stability and are, by far, the most commonly employed magnetic nanoparticles for biomedical applications [32-34].

Two different strategies can be employed to produce magnetic polyelectrolyte nanocarriers: i) to place magnetic nanoparticles inside the capsules core [35, 36] or ii) to incorporate them in the polyelectrolyte shell [37-40]. The latter has the additional advantage of enabling triggered release of a cargo by external magnetic field. In ~~the~~ a previous paper [41] we demonstrated the feasibility of formation of nanocapsules with the size of 150 nm by the layer-by-layer adsorption of biocompatible polyelectrolytes with the single layer formed of Fe_3O_4 nanoparticles. In this work we ~~produced~~ propose a nanosystems that could combine hyperthermia cancer treatment and magnetically triggered release of encapsulated drugs. It ~~was~~ is based on magnetic nanocapsules, of the size in the range of 100-200 nm, with one or two Fe_3O_4 layers in the polyelectrolyte shell ~~formed~~ obtained by the LbL technique with polycation/polyanion pair with proven biocompatibility, i.e., poly-L-lysine hydrobromide/poly-L-glutamic acid sodium salt. We demonstrate~~d~~ their magnetic response and ~~tested them for~~their possibility ~~of the~~to combine~~d~~ hyperthermia and drug delivery applications.

Experimental

Chemicals

The aqueous suspension of Fe_3O_4 nanoparticles without organic stabilizer (8 ± 3nm, for the LbL applications) was obtained from PlasmaChem GmbH Berlin, Germany. The polycation poly-L-lysine hydrobromide, PLL (MW ~15000 to 30000) and polyanion: poly-L-glutamic acid sodium salt, PGA (MW ~15000 to 50000), docusate sodium salt (AOT), chloroform and sodium chloride were obtained from Sigma-Aldrich. All materials were used as received without further purification. Pegylated polyelectrolyte (PGA-g-PEG) was synthesized in our lab according to the protocol [13] by coupling PEG chains to PGA backbone. The coupling rate was approximately 40% and that resulting polymer was referred to as PGA-g-PEG. The ultrapure water was obtained using the Millipore Direct-Q5 UV purification system.

Synthesis of nanocapsules

The nanocapsules were prepared according to the protocol described before [41] i.e. by encapsulation of emulsion droplets in the hybrid polyelectrolyte shell. The general scheme for the formation of magnetically responsive nanocapsules is illustrated in Figure 1. Nanoemulsion droplets were stabilized by the interfacial (surfactant AOT)/(polycation PLL) complex as it was described by Szczepanowicz et al. [14]. The nanoemulsion preparation conditions were optimized by selection of proper AOT/PLL ratio. Nanoemulsion droplets were formed by addition of an oil phase to polycation (PLL) solution during mixing with a magnetic stirrer at 300 rpm. The oil phase for the emulsification was prepared by dissolving anionic surfactant AOT in chloroform at the concentration 340g/l. All polyelectrolytes were dissolved in NaCl solutions of ionic strength 0.015 M, to obtain polyelectrolyte solution of concentration 2 g/l at natural pH, i.e., without pH adjustment. After formation of stable nanoemulsion drops stabilized by the AOT/PLL interfacial complex the hybrid multilayer shell was constructed by the saturation method of the layer by layer technique [6] i.e., by the subsequent adsorption of polyelectrolytes/nanoparticles from their solutions without the intermediate rinsing step. A fixed volume of nanoemulsion/nanocapsules was added to the oppositely charged polyelectrolyte solution or Fe_3O_4 nanoparticles during continuous shaking and the shell formation was followed by the zeta potential measurements. Shaking was used instead of mixing by magnetic stirring to avoid aggregation/agglomeration of magnetic species on magnetic stirrers. The procedure of sequential deposition of polyelectrolytes and nanoparticles layers was repeated until an appropriate number of layers in the hybrid multilayer shell was formed. To create pegylated nanocapsules, PLL-terminated hybrid nanocapsules with five or seven layers were coated with the layer of PGA-*g*-PEG using the same procedure as described above. For the sake of clarity, we denote them as NCn – the nanoemulsion encapsulated by n polyelectrolyte layers (NC1 corresponds to the drops with AOT/PLL surface complex). Because of the toxicity issue, chloroform was evaporated from suspensions of nanocapsules shortly after preparation. The amount of the chloroform after evaporation was determined as not exceeding 0.04 mg/l [42].
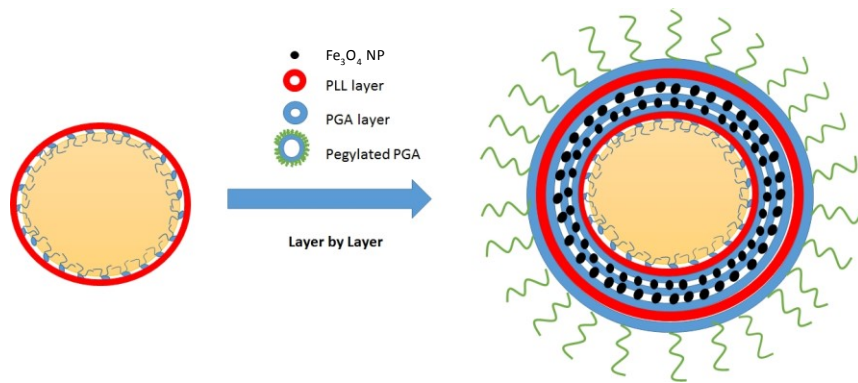
Figure 1: Scheme of the formation of magnetically responsive nanocapsules for biomedical application

Characterization of nanocapsules

Size, concentration and zeta potential determination

The hydrodynamic diameter (size) of nanocapsules was determined by Dynamic Light Scattering (DLS). Zeta potential of polyelectrolytes and nanoparticles/nanocapsules was determined by the microelectrophoretic method, both using Malvern Instruments Zetasizer Nano ZS. Additionally, the concentration of nanocapsules was determined by the Nanoparticle Tracking Analysis (NTA) technique with the NS500 instrument (NanoSight). All measurements were performed in 0.015M NaCl at 25°C.

Stability tests

Freshly prepared suspensions of nanocapsules were stored in 0.015M NaCl and cell culture media containing 10% FBS. To evaluate the colloidal and biological stability of the nanocapsules, the size distribution of the nanocapsules were monitored in time.

Magnetic heating

The capability of the magnetically loaded capsules to develop heat under the application of rf magnetic fields was tested by means of a DM100 nanoScale Biomagnetics apparatus for the measurement of magnetic hyperthermia. In particular, 0.5ml batches of capsule samples were irradiated using a magnetic field of 25 mT oscillating with a frequency of 429 kHz. The temperature of the sample was

followed as a function of time by means of an optical fiber thermometer with a temperature sensitivity of ~0.1 °C. The heating rates (HR) have been obtained from the raw data by fitting the temperature increase at early times, up to 300 sec, with a linear dependence. The departure from the linearity at longer times and the saturation value of the temperature increase are dictated by the combined effects of heating power and thermal losses.

Nanocapsules structure

SEM and Cryo-SEM

For the cryo-SEM imaging, a small droplet of a capsule's suspension was put on the cold holder. The sample holder was attached to a transfer rod and immediately immersed (frozen) in the liquid nitrogen slush using the Quorum PPT2000 cryo-preparation stage (Polaron, Quorum Technologies, UK). The holder with the frozen sample was raised and cryo-transferred at the temperature of liquid nitrogen vapors to the chamber of the cryo-unit where the sample was subjected to sublimation at −70°C for 15–30 min. (until all visible ice crystals disappeared). The sample was then sputter coated with platinum (5 nm thickness). Following coating, the specimen was transferred to the cooled stage of the Jeol JSM 7600F field emission scanning electron microscope FESEM (Jeol Ltd., Tokyo, Japan).

More SEM images have been obtained also by using a ZEISS Field-Emission SUPRA40 electron microscope equipped with a GEMINI FESEM detection column operating at 10keV on samples prepared on silicon substrates.

AFM

AFM imaging was performed in air, at room temperature, using either a Thermomicroscope CP research or a Park XE 100 AFM microscope, both equipped with a high-resolution 5μm scanner, with Bruker/Veeco MLCT or NT-MDT Etalon tips. The sample was prepared by drying in ambient conditions a drop of suspension on a freshly cleaved mica substrate.

Results and Discussion

Magnetically responsive nanocapsules' preparation

For the optimization of nanoemulsion preparation conditions, concentration of PLL was varied from 50 to 400ppm, while the volume of the oil phase was fixed. The optimal ratio of AOT/PLL concentrations was determined by measuring the zeta potential of emulsion nanodrops and by evaluating their stability. It corresponded to the value of zeta potential (+60 ±5mV) reached before the overcharging, as indicated in Figure 2a, which shows the dependence of the zeta potential on the concentration of polyelectrolyte solution used to form the nanoemulsion cores. In those conditions, the amount of unabsorbed polycation was minimized as most of it was adsorbed at the emulsion droplets. The average drop size of nanoemulsion droplets stabilized by AOT/PLL complex (NC1), measured by DLS, was around 50 nm with polydispersity index (PDI) <0.3. The high value of zeta potential of NC1 indicated that the surface charge was high enough to provide the electrostatic stabilization, therefore the nanoemulsion was suitable for the LbL adsorption process. Thus, such prepared nanoemulsion droplets were further encapsulated in hybrid multilayer shell using the saturation method. For the formation of the shell, biocompatible components were used: PGA as the anionic component and PLL or Fe_3O_4 as the cationic components. Fixed volume of positively charged nanoemulsion (NC1) was added to the PGA solutions (2g/l 0,015M NaCl) under mechanical stirring, to form a second polyelectrolyte layer. The amount of polyanion used to form stable anionic layer (NC2) was chosen empirically, analyzing the results of simultaneous zeta potential measurements: the optimal amount of PGA (marked by asterisks on Figure 2b) corresponded to the saturated polyelectrolyte layer formed on nanoemulsion droplets (NC2), while the amount of unabsorbed PGA in the capsules suspension was minimized as most of it was consumed to reverse charge of nanocapsules and to form the PGA layer of capsules shell. Given the positive zeta potential of Fe_3O_4 nanoparticles (+45mV), they were used as third layer in the multilayer structure. Fixed volume of NC2 nanocapsules (PGA terminated) was added to Fe_3O_4 nanoparticle suspension during continuous shaking. The amount of Fe_3O_4 nanoparticles suspension used to form a stable saturated third layer was chosen empirically by analyzing the simultaneous zeta potential measurements (as it was done for the polyelectrolyte layers). The optimal amount of Fe_3O_4 nanoparticles (marked by the asterisk in Figure 2c) corresponds to the conditions when the zeta potential of the nanocapsules reached a value close to the zeta potential of the Fe_3O_4 nanoparticles in solution, just before overcharging the capsules; this indicates the formation of saturated layer. The next layers in the hybrid multilayer shell were formed by repeating the procedure described above. Figure 3

illustrates the dependence of the zeta potential of capsules on the adsorption of subsequent layers; the typical saw-like pattern is an evidence of the formation of a multilayer shell. For further experiments, two types of nanocapsules were selected: NC4 with the shell composition $AOT/PLL/PGA/Fe_3O_4/PGA$- i.e. with one layer of magnetic nanoparticles-, and NC6 with shell composition $AOT/PLL/PGA/Fe_3O_4/PGA/Fe_3O_4/PGA$ – i.e. with two layers formed by magnetic nanoparticles.
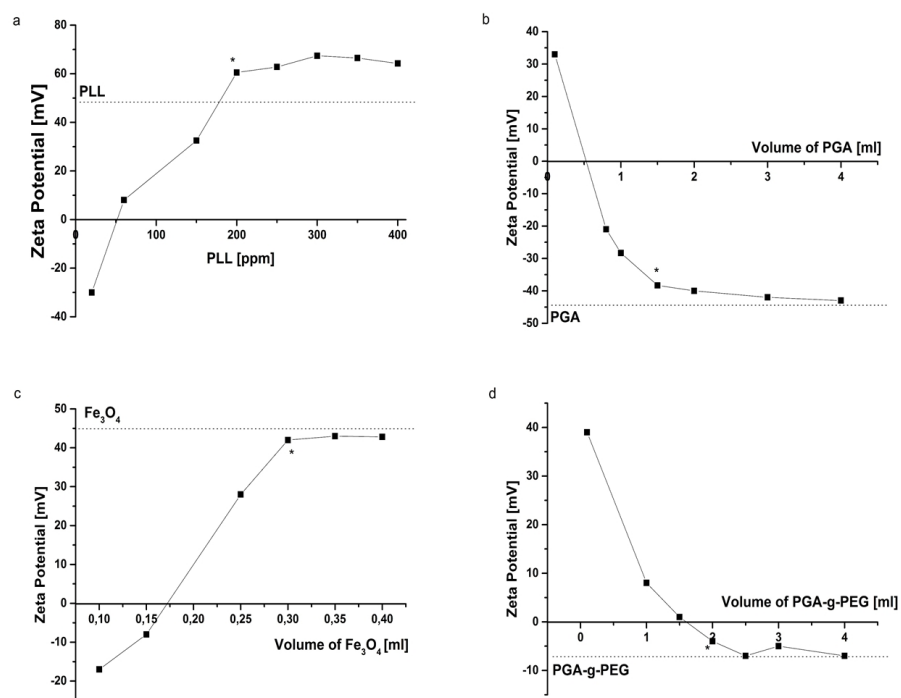

Figure 2: Changes of the zeta potential of a) emulsion cores (NC1) with the various PLL concentration used for emulsification b) NC2 nanocapsules with various volume of PGA used to form saturated layer; (c) NC3 capsules with various volume of Fe_3O_4 used to form saturated layer; (d) pegylated nanocapsules with various volume of PGA-g-PEG used during formation of pegylated layer. In all panels, an asterisk marks the first stable sample before overcharging. Horizontal lines correspond to the zeta potential of polyelectrolytes/nanoparticles in solution.
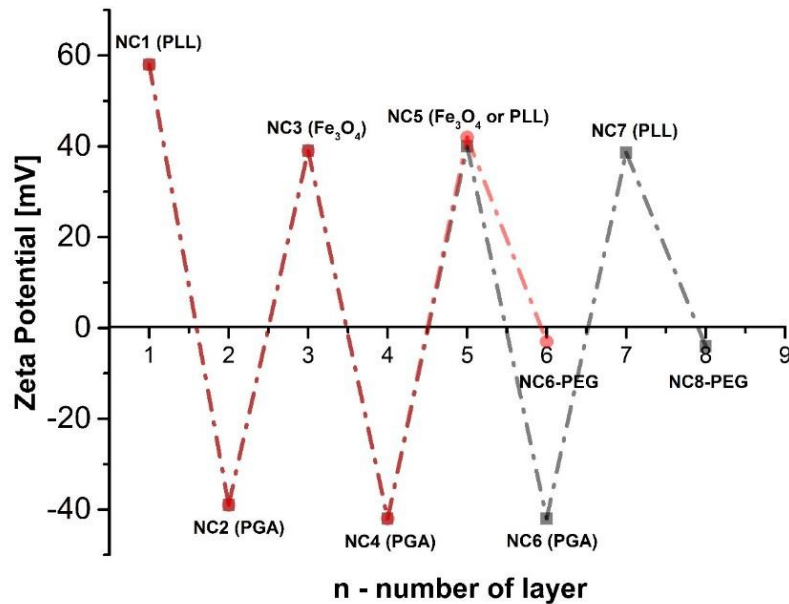
Figure 3: The saw-like dependence of zeta potential on the number of deposited layers during formation of hybrid polyelectrolyte shell with embedded magnetic nanoparticles.

Pegylation of magnetically responsive nanocapsules for biomedical applications

Biomedical application of nanocarriers requires their specific modification in order to exclude recognition by mononuclear phagocytic system and avoid fast clearance, which reduces the circulating half-life and therefore limits the effectiveness of nanoparticles as drug delivery system. Pegylation is one of the available methods to prevent serum protein adsorption and non-specific bindings that promote fast phagocytosis [43]. The pegylated nanocapsules were synthesized according to the strategy described earlier [13], by using pegylated polyanion PGA-g-PEG as an external layer in multilayer shell. For the preparation of pegylated nanocapsules, an additional PLL layer was formed on NC4 and NC6

nanocapsules, while PLL-terminated nanocapsules with five or seven polyelectrolyte layers (NC5 or NC7) were coated with pegylated PGA (PGA-g-PEG) to form pegylated nanocapsules (NC6-PEG and NC8-PEG), using the same procedure as for a normal saturated polyelectrolyte layer. The optimal volume of PGA-g-PEG used to form stable saturated pegylated external layer was determined by monitoring the zeta potential of nanocapsules, i.e. when it reached a value similar to pegylated PGA in solution, c.a. 0 mV. The optimal condition for the formation of saturated pegylated external layer was marked by an asterisk in Figure 2d.

Magnetic nanoparticles' characterization

For an effective incorporation in the polyelectrolyte shell, iron oxide nanoparticles should be well monodisperse and stable in water. The size distribution and morphology of the Fe_3O_4 nanoparticles were measured by DLS and SEM microscopy. DLS experiments performed in water at RT, gave correlation functions whose Q-dependent decay corresponded to a hydrodynamic radius of 9-10 nm with low polydispersity. Using SEM microscopy, we acquired high resolution images of a highly diluted suspension of nanoparticles dispersed and dried on a clean silicon substrate. Figure 4, left panel, shows a typical SEM micrograph. From these images, we derived a statistical analysis of the size distribution of magnetite nanoparticles. The results are shown in the right panel of Figure 4. This distribution was fitted with a log normal distribution, with mean nanoparticles diameter of 10.7±1.6 nm. This value agrees well with the size measured by DLS as well with the nominal size specified by the supplier. The nanometric size of these particles is compatible with a superparamagnetic behavior at Room Temperature [44], being well below the superparamagnetic blocking size at RT for magnetite (d=26nm) [45].
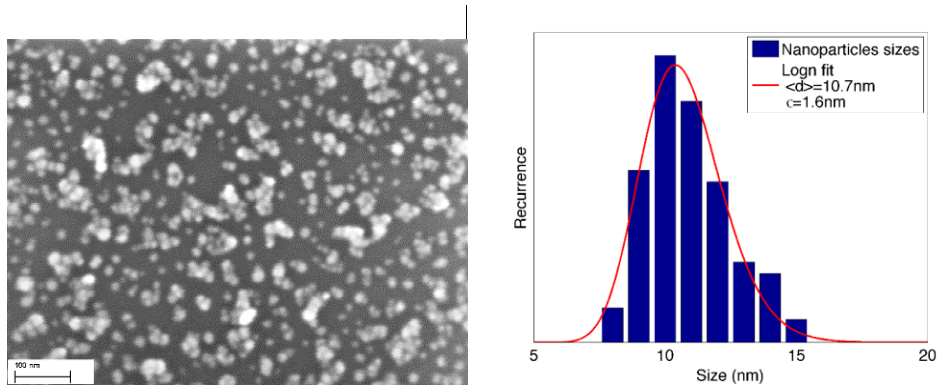
Figure 4: SEM characterization of magnetite nanoparticles. Left panel: SEM micrograph of the bare magnetite nanoparticles. Right panel: the corresponding histogram of the size distribution, fitted with a lognormal distribution (red line).

Nanocapsules' characterization

The CRYO- SEM Micrographs of the NC4 and NC6 nanocapsules are shown in Figure 5. Most of the observed particles have size below 100 nm, which is in good agreement with the values obtained by DLS, collected in Table 1. Particle concentration in the stock solution after synthesis, determined by NTA, was ~1.1×10^{12} and ~4.8×10^{10} nanocapsules/ml for NC4 and NC6 nanocapsules respectively. Zeta potential values of hybrid nanocapsules ranging from below ~−40 mV for the polyanion layers to above ~+40 mV for the polycation layers indicate that the surface charge of particles is adequate to prevent nanocapsule aggregation and to ensure their long-term stability. We did not observe significant changes in size and zeta potential of prepared capsules for up to 90 days (stored and measured in 0,015M NaCl). Pegylation of nanocapsules ensured their stability (up to 90 days) in physiological conditions (0.15M NaCl) due to the steric stabilization mechanisms (zeta potential close to 0 mV) that has been demonstrated in Figure 6. The stability studies of pegylated nanocapsules in a cell culture medium containing fetal bovine serum (FBS) solution were also performed. We found that pegylated nanocapsules retained their size and zeta potential without significant changes for at least 48 hours. The long-term stability of nanocapsules together with their biocompatibility is an important prerequisite for any pharma-application.
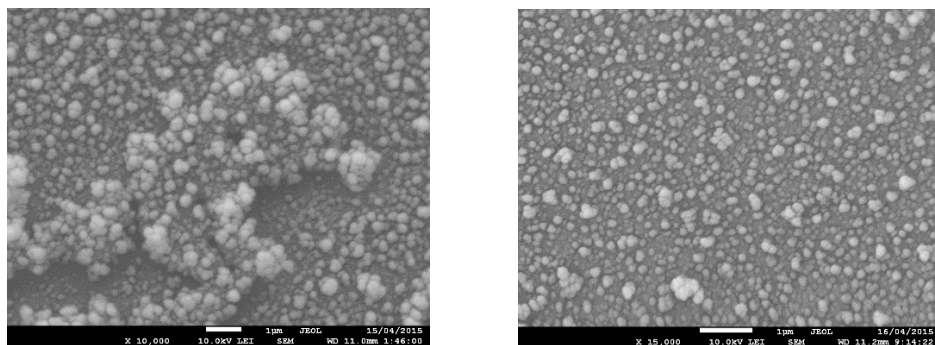
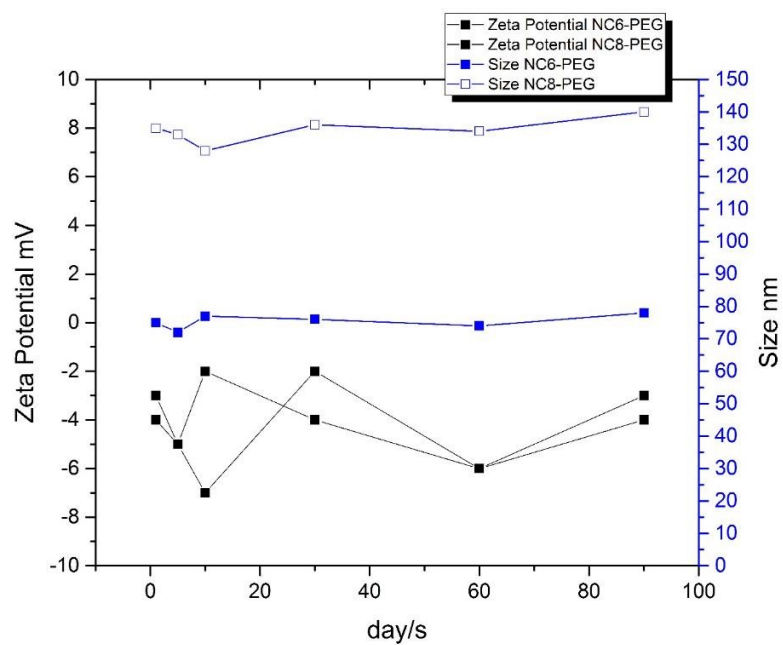**Figure 5**: Cryo-SEM images of NC4 (left) and NC6 (right) nanocapsules.

Figure 6: Stability studies of pegylated hybrid nanocapsules, size and zeta potential measurements with time.

Magnetic properties

A proof of concept of the delivery capacity of the nanocapsules was shown in Figure 7, where they were attracted by the magnetic field gradient generated by a permanent magnet [46]. Four cuvettes containing hybrid nanocapsules suspensions (NC4 and NC6) were placed next to each other; the magnets were placed close to two of them. At the beginning of the experiment nanocapsules distributions were homogeneous in all cases. After a few hours, nanocapsules NC4 and NC6 were concentrated at the side of the cuvette located next to the magnet and the residual liquid became transparent. The distribution of the hybrid nanocapsules in cuvettes without the magnets remained unchanged. These results prove that the changes in nanocapsules distribution in the cuvettes were due to the magnetic field.
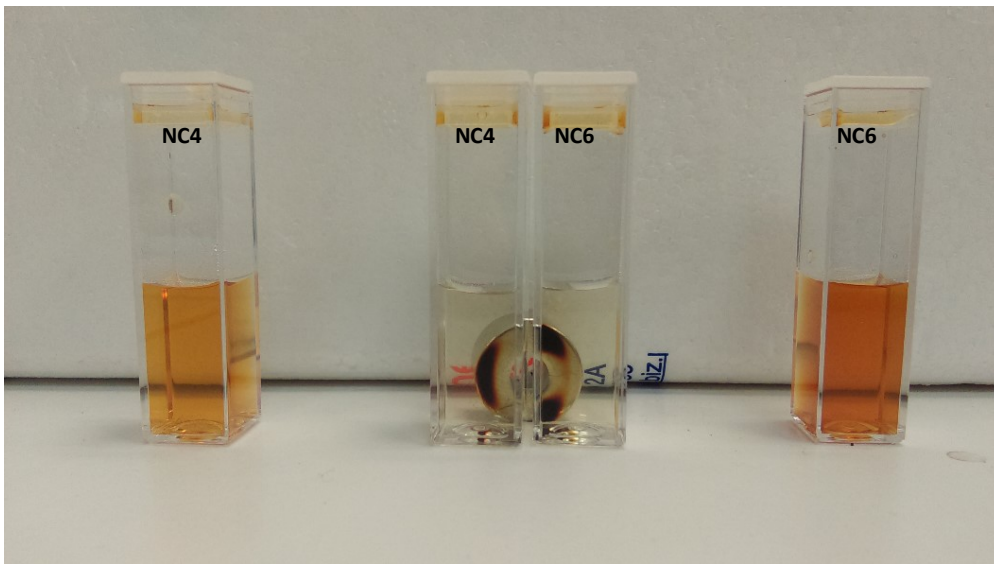

Figure 7: Nanocapsules suspension attracted by magnetic field. The magnet was placed close to the two cuvettes in the middle. Change in the distribution of hybrid nanocapsules was only observed for the cuvettes located next to the magnet.

The effect of alternating magnetic field on nanocapsules suspension was investigated for samples NC4, NC6 and NC4d. The last is obtained from the NC4 suspension by diluting it with 0,015M NaCl to reach the same volume concentration (in nanocapsules/ml) as in NC6. Tested suspensions contain

5×10^{-4} g/ml, 5.34×10^{-4} g/ml and 2.14×10^{-5} g/ml of Fe_3O_4 nanoparticles in NC4, NC6 and NC4d nanocapsules suspensions. The increase in the temperature of the samples during radio frequency (rf) magnetic field irradiation was observed and reported in Figure 8. By fitting the temperature increase ΔT with a linear trend at early times, up to 300s (continuous lines), the heating rate HR of each sample was determined. The deviation from linearity at longer times and the saturation value of the temperature increase are dictated by the combined effects of heating power and thermal losses. From the comparison of the heating rates of NC6 and NC4d -i.e. for the same concentration of nanocapsules but with two and one iron oxide layers in the shell- one can conclude that NC6 capsules are much more effective for hyperthermia. This can be explained by the higher amount of Fe_3O_4 nanoparticles that was necessary to add to the nanocapsules to form the second layer, as well as by the possible aggregation of magnetic nanoparticles within the shell. On the other hand, the heat effect for NC4 and NC6 is similar, though the number of nanocapsules is 1.5 order of magnitude lower in the latter case. This suggest that heating rates roughly scale with the content of iron oxide content.
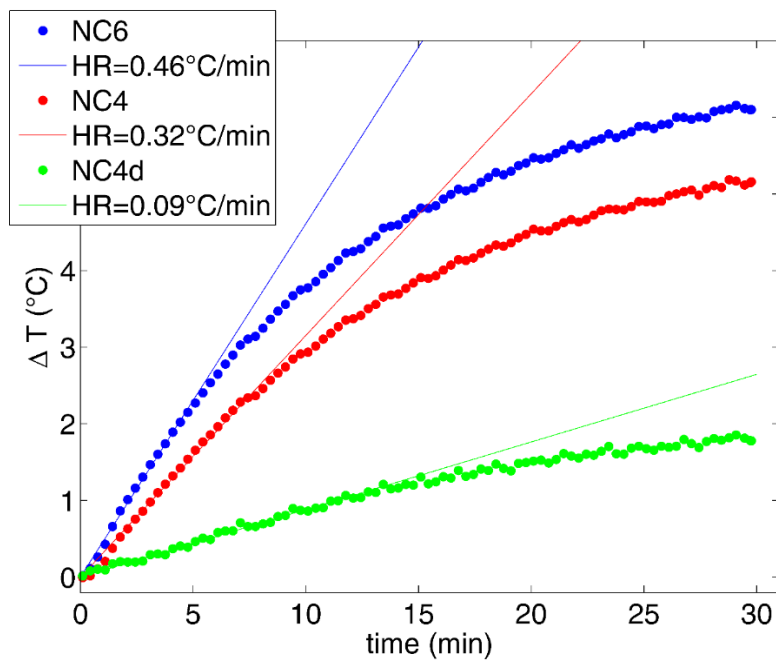
Figure 8: Increase of temperature in NC4, NC6 and NC4d nanocapsules suspension during rf magnetic field irradiation. Continuous lines are the linear fits at early time (up to 5min) from which heating rates HR are extracted.

To detect any change in capsule morphology, we performed DLS measurements on both irradiated and control samples. The results for size of NC4 and NC6 nanocapsules are reported in Figure 9. The left panels, a) and c) report the correlation functions (c.f.) of samples NC4 and NC6 respectively. For each sample, we characterized the size of a control batch (black lines) and a batch irradiated with rf magnetic field (color lines). We found that the c.f. corresponding to the irradiated samples decay at larger characteristic times than the corresponding controls: this proved that rf-irradiation caused an increase in the size of the capsules.
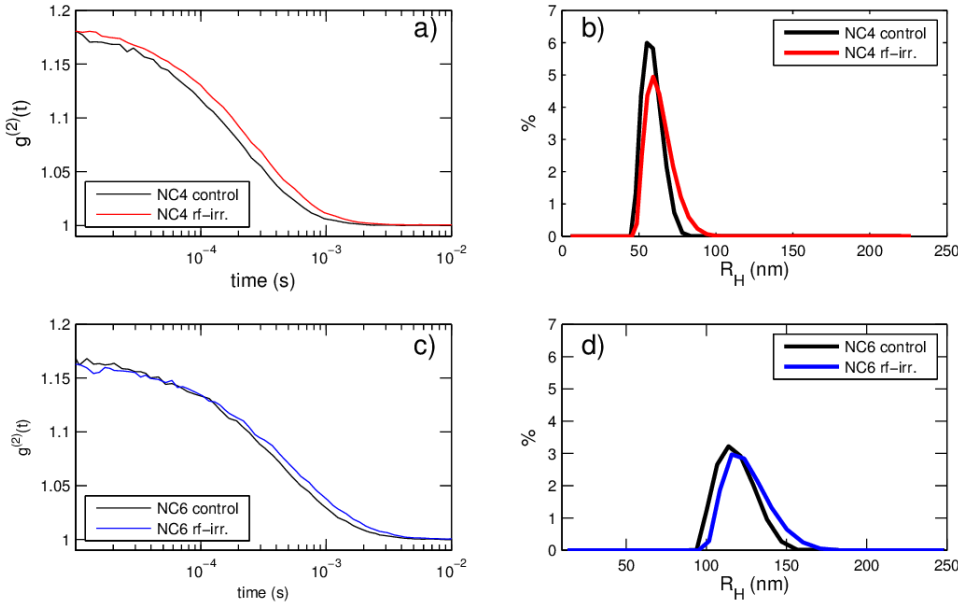

Figure 9: Irradiation with rf magnetic field causes an increase in the average hydrodynamic radius of the capsules, as measured by DLS. Panels a) and c) reports the correlation functions of samples NC4 and NC6 respectively, measured before (black lines) and after (color lines) irradiation. Panels b) and d)

reports the corresponding number-weighted size distributions obtained through an analysis performed using the CONTIN Inverse Laplace algorithm.

From the correlation functions, we extract the corresponding number-weighted size distributions through the CONTIN Inverse Laplace algorithm [47]. The resulting size distributions are illustrated in panels b) and d) for samples NC4 and NC6 respectively, following the same color scheme of panels a) and c) to indicate control or irradiated samples. Average radius and standard deviation of the distributions of the control and rf- irradiated samples were obtained from a Gaussian fitting of the peaks and the values are collected in Table 1. The average radius consistently increased upon irradiation: NC4 by 8% and NC6 by 6% respectively, while the standard deviation of size distribution grew fourfold. These results indicate the existence of a morphological effect induced on the capsules by rf irradiation.

	$\overline{R_H}$ (nm)	σ (nm)
NC4 control	58.8 ± 0.5	6.3 ± 0.5
NC4 rf irradiated	63.6 ± 0.5	8.6 ± 0.5
NC6 control	119 ± 2	12 ± 2
NC6 rf irradiated	126 ± 2	14 ± 2

Table 1: Average hydrodynamic radius and standard deviation of the size distributions of samples NC4 and NC6, obtained by a Gaussian fit of the data.

To better elucidate this effect, we performed AFM microscopy investigations. Samples were prepared by dispersing an aliquot of suspension on a freshly cleaved mica surface, and left drying in ambient. In Figure 10 we report a typical AFM image of NC6 nanocapsules. In the left panel, the pristine sample, in which a rough estimate of the size confirms the value found by DLS (about 100 nm). On the contrary, the irradiated sample (right panel) is characterized by the presence of debris and fragments, which appear isolated and spread on wide areas or aggregated into thin, long stripes. This observation suggests that rf-treatment induced capsule opening and fragmentation.
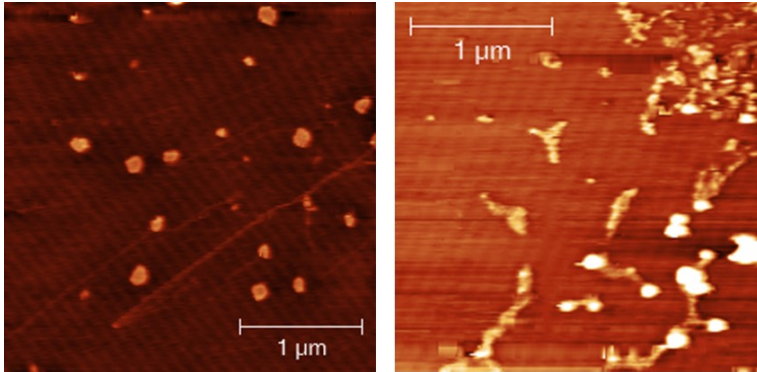
Figure 10: AFM images show that irradiation with rf magnetic fields affects the morphology of the sample. Left: AFM image of pristine NC6 nanocapsules on a freshly cleaved mica surface. The round features correspond to individual capsules. Right: NC6 irradiated sample.

The nanocapsules presented in this work have shown to possess the key properties for their application ~~in a therapy~~in treatments that combine~~s~~ hyperthermia and drug delivery [F. Ridi, M. Bonini, and P. Baglioni, Adv. Colloid Interface Sci. 207, 3 (2014)]. The inclusion of ~~layers formed by~~ magnetic nanoparticles in the shell of the nanocapsules ensures that i) they can be guided by external ~~static~~ magnetic fields to reach, after injection, the desired location inside the body (Figure 7), ii) they induce an increase of temperature in their vicinity when irradiated by rf magnetic fields, which is roughly proportional to the <u>amount</u> of magnetic nanoparticles included in the shell (Figure 8), iii) the same rf irradiation opens the capsules, thus leading to the triggered release of the nanocapsules load in the desired position (Figures 9-10). We remark here that this ~~two~~<u>double</u>-side~~d~~ response is triggered simultaneously by the same external trigger, a rf magnetic field, which is characterized by higher penetration and lower invasiveness if compared to other stimuli such as UV or IR light.

The nanometric size of the platform is a key point in view of its effectiveness in applications, ensuring high~~er~~ diffusivity and enhancing cellular uptake; despite the small size, the nanocapsules presented in this work show heating rates upon irradiation and drug-release capabilities comparable with those of much larger platforms. We compare their hyperthermia efficiency to that of similar LbL-assembled polyelectrolyte microcapsules with iron oxide nanocubes integrated in their walls [S. Carregal-Romero,

P. Guardia, X. Yu, R. Hartmann, T. Pellegrino, and W. J. Parak, Nanoscale **7**, 570 (2015)]; they are micrometric in size and incorporate in their shell 18nm iron oxide nanocubes. The capsules of ref [Carregal-Romero] show an heating rate of 29°C/min with a concentration of iron nanoparticles 10 times higher than in our NC6 sample; if normalized to the iron content, that rate is comparable with the 0.46°C/min rate of the NC6 sample observed in similar irradiation conditions, despite the major differences in size of the capsule and of the iron-oxide nanoparticles.

> **Commentato [TR1]:** Lo toglierei perchè è già detto sopra…

Conclusions

Magnetically responsive nanocapsules with hybrid polyelectrolyte/Fe$_3$O$_4$ nanoparticles were successfully prepared. They were ~~formed~~ obtained from nanoemulsion core and biocompatible polyelectrolyte (PLL and PGA) multilayer shell with embedded superparamagnetic Fe$_3$O$_4$ nanoparticles. Furthermore, nanocapsules were modified for biomedical application by pegylation, which should make them invisible for phagocytic cells [43]. Our magnetically responsive nanocapsules can be guided to and can be concentrated at the target disease area by the magnetic field; moreover, they can be useful for magnetic hyperthermia ~~therapy~~ treatment since they can generate heat in an alternating magnetic field. The AFM and DLS measurements indicate morphological changes of the nanocapsules induced by the alternating rf magnetic field that suggest that encapsulated cargo could be ~~triggered~~ released on-demand by alternating magnetic field irradiation. Thus, considering their size and magnetic properties, our nanocapsules may considered as a promising tool for future medical application e.g. cancer treatment.

Acknowledgements

References

(1) Viet Long, N.; Minh Thi, C.; Yong, Y.; Cao, Y.; Wu, H.; Nogami, M. Synthesis and Characterization of Fe-Based Metal and Oxide Based Nanoparticles: Discoveries and Research Highlights of Potential Applications in Biology and Medicine. *Recent patents on nanotechnology* **2014**, *8*, 52-61.

(2) Ruiz-Molina, D.; Novio, F.; Roscini, C. In *Bio-and Bioinspired Nanomaterials;* John Wiley & Sons: 2014; .

(3) Dewey, W.; Hopwood, L.; Sapareto, S.; Gerweck, L. Cellular Responses to Combinations of Hyperthermia and Radiation 1. *Radiology* **1977**, *123*, 463-474.

(4) Langer, R. Drug Delivery and Targeting. *Nature* **1998**, *392*, 5-10.

(5) Torchilin, V. P. In *Passive and active drug targeting: drug delivery to tumors as an example;* Drug delivery; Springer: 2010; pp 3-53.

(6) Sukhorukov, G. B.; Donath, E.; Lichtenfeld, H.; Knippel, E.; Knippel, M.; Budde, A.; Möhwald, H. Layer-by-Layer Self Assembly of Polyelectrolytes on Colloidal Particles. *Colloids Surf. Physicochem. Eng. Aspects* **1998**, *137*, 253-266.

(7) Voigt, A.; Lichtenfeld, H.; Sukhorukov, G. B.; Zastrow, H.; Donath, E.; Baumler, H.; Mohwald, H. Membrane Filtration for Microencapsulation and Microcapsules Fabrication by Layer-by-Layer Polyelectrolyte Adsorption. *Ind Eng Chem Res* **1999**, *38*, 4037-4043.

(8) Borodina TN, Rumsh LD, Kunizhev SM, Sukhorukov GB, Vorozhtsov GN, Feldman BM, Markvicheva EA. Polyelectrolyte Microcapsules as Systems for Delivery of Biologically Active Substances. *Biomed Khim.* **2007**, *53*, 557-565.

(9) Erokhina, S.; Berzina, T.; Cristofolini, L.; Erokhin, V.; Folli, C.; Konovalov, O.; Marino, I.; Fontana, M. X-Ray Reflectivity Measurements of Layer-by-Layer Films at the Solid/Liquid Interface. *Langmuir* **2008**, *24*, 12093-12096.

(10) Parakhonskiy, B. V.; Yashchenok, A. M.; Konrad, M.; Skirtach, A. G. Colloidal Micro- and Nano-Particles as Templates for Polyelectrolyte Multilayer Capsules. *Adv. Colloid Interface Sci.* **2014**, *207*, 253-264.

(11) Guzey, D.; McClements, D. J. Formation, Stability and Properties of Multilayer Emulsions for Application in the Food Industry. *Adv. Colloid Interface Sci.* **2006**, *128–130*, 227-248.

(12) Grigoriev, D. O.; Bukreeva, T.; Mohwald, H.; Shchukin, D. G. New Method for Fabrication of Loaded Micro- and Nanocontainers: Emulsion Encapsulation by Polyelectrolyte Layer-by-Layer Deposition on the Liquid Core. *Langmuir* **2008**, *24*, 999-1004.

(13) Szczepanowicz, K.; Hoel, H. J.; Szyk-Warszynska, L.; Bielanska, E.; Bouzga, A. M.; Gaudernack, G.; Simon, C.; Warszynski, P. Formation of Biocompatible Nanocapsules with Emulsion Core and Pegylated Shell by Polyelectrolyte Multilayer Adsorption. *Langmuir* **2010**, *26*, 12592-12597.

(14) Szczepanowicz, K.; Dronka-Góra, D.; Para, G.; Warszynski, P. Encapsulation of Liquid Cores by Layer-by-Layer Adsorption of Polyelectrolytes. *J. Microencapsulation* **2010**, *27*, 198-204.

(15) Piotrowski, M.; Szczepanowicz, K.; Jantas, D.; Leskiewicz, M.; Lason, W.; Warszynski, P. Emulsion-Core and Polyelectrolyte-Shell Nanocapsules: Biocompatibility and Neuroprotection Against SH-SY5Y Cells. *J. Nanopart. Res.* **2013**, *15*.

(16) Adamczak, M.; Krok, M.; Pamula, E.; Posadowska, U.; Szczepanowicz, K.; Barbasz, J.; Warszynski, P. Linseed Oil Based Nanocapsules as Delivery System for Hydrophobic Quantum Dots. *Colloids Surf. B Biointerfaces* **2013**, *110*, 1-7.

(17) Karabasz, A.; Bzowska, M.; Lukasiewicz, S.; Bereta, J.; Szczepanowicz, K. Cytotoxic Activity of Paclitaxel Incorporated into Polyelectrolyte Nanocapsules. *J. Nanopart. Res.* **2014**, *16*.

(18) Szczepanowicz, K.; Podgórna, K.; Szyk-Warszynska, L.; Warszynski, P. Formation of Oil Filled Nanocapsules with Silica Shells Modified by Sequential Adsorption of Polyelectrolytes. *Colloids Surf. A Physicochem. Eng. Asp.* **2014**, *441*, 885-889.

(19) Adamczak, M.; Kupiec, A.; Jarek, E.; Szczepanowicz, K.; Warszynski, P. Preparation of the Squalene-Based Capsules by Membrane Emulsification Method and Polyelectrolyte Multilayer Adsorption. *Colloids Surf. A Physicochem. Eng. Asp.* **2014**, *462*, 147-152.

(20) Plawecka, M.; Snihirova, D.; Martins, B.; Szczepanowicz, K.; Warszynski, P.; Montemor, M. F. Self Healing Ability of Inhibitor-Containing Nanocapsules Loaded in Epoxy Coatings Applied on Aluminium 5083 and Galvanneal Substrates. *Electrochim. Acta* **2014**, *140*, 282-293.

(21) Szczepanowicz, K.; Bazylinska, U.; Pietkiewicz, J.; Szyk-Warszynska, L.; Wilk, K. A.; Warszynski, P. Biocompatible Long-Sustained Release Oil-Core Polyelectrolyte Nanocarriers: From Controlling Physical State and Stability to Biological Impact. *Adv. Colloid Interface Sci.* **2015**, *222*, 678-691.

(22) Mu, B.; Liu, P.; Du, P.; Dong, Y.; Lu, C. Magnetic-Targeted pH-Responsive Drug Delivery System Via Layer-by-Layer Self-Assembly of Polyelectrolytes Onto Drug-Containing Emulsion Droplets and its Controlled Release. *Journal of Polymer Science Part A: Polymer Chemistry* **2011**, *49*, 1969-1976.

(23) Ai, H. Layer-by-Layer Capsules for Magnetic Resonance Imaging and Drug Delivery. *Adv. Drug Deliv. Rev.* **2011**, *63*, 772-788.

(24) Zebli, B.; Susha, A. S.; Sukhorukov, G. B.; Rogach, A. L.; Parak, W. J. Magnetic Targeting and Cellular Uptake of Polymer Microcapsules Simultaneously Functionalized with Magnetic and Luminescent Nanocrystals. *Langmuir* **2005**, *21*, 4262-4265.

(25) Allen, T. M.; Cullis, P. R. Drug Delivery Systems: Entering the Mainstream. *Science* **2004**, *303*, 1818-1822.

(26) Gupta, A. K.; Gupta, M. Synthesis and Surface Engineering of Iron Oxide Nanoparticles for Biomedical Applications. *Biomaterials* **2005**, *26*, 3995-4021.

(27) Gupta, A. K.; Naregalkar, R. R.; Vaidya, V. D.; Gupta, M. Recent Advances on Surface Engineering of Magnetic Iron Oxide Nanoparticles and their Biomedical Applications. Nanomedicine **2007**, 2, 23-39.

(28) Duguet, E.; Vasseur, S.; Mornet, S.; Devoisselle, J. Magnetic Nanoparticles and their Applications in Medicine. Nanomedicine **2006**, 1, 157-168.

(29) McCarthy, J. R.; Kelly, K. A.; Sun, E. Y.; Weissleder, R. Targeted Delivery of Multifunctional Magnetic Nanoparticles. Nanomedicine **2007**, 2, 153-167.

(30) Serrano- Ruiz, D.; Laurenti, M.; Ruiz- Cabello, J.; López- Cabarcos, E.; Rubio-Retama, J. Hybrid Microparticles for Drug Delivery and Magnetic Resonance Imaging. *Journal of Biomedical Materials Research Part B: Applied Biomaterials* **2013**, *101*, 498-505.

(31) Ozdemir, V.; Williams-Jones, B.; Glatt, S. J.; Tsuang, M. T.; Lohr, J. B.; Reist, C. Shifting Emphasis from Pharmacogenomics to Theragnostics. *Nature* **2006**, *200*, 1.

(32) Ito, A.; Shinkai, M.; Honda, H.; Kobayashi, T. Medical Application of Functionalized Magnetic Nanoparticles. *Journal of bioscience and bioengineering* **2005**, *100*, 1-11.

(33) Shubayev, V. I.; Pisanic, T. R.; Jin, S. Magnetic Nanoparticles for Theragnostics. *Adv. Drug Deliv. Rev.* **2009**, *61*, 467-477.

(34) Tartaj, P.; del Puerto Morales, M.; Veintemillas-Verdaguer, S.; González-Carreño, T.; Serna, C. J. The Preparation of Magnetic Nanoparticles for Applications in Biomedicine. *J. Phys. D* **2003**, *36*, 13.

(35) Veyret, R.; Delair, T.; Elaissari, A. Preparation and Biomedical Application of Layer-by-Layer Encapsulated Oil in Water Magnetic Emulsion. *J Magn Magn Mater* **2005**, *293*, 171-176.

(36) Podgórna, K.; Szczepanowicz, K. Synthesis of Polyelectrolyte Nanocapsules with Iron Oxide (Fe 3 O 4) Nanoparticles for Magnetic Targeting. *Colloids Surf. Physicochem. Eng. Aspects* **2016**.in press

(37) Caruso, F.; Susha, A. S.; Giersig, M.; Möhwald, H. Magnetic Core?Shell Particles: Preparation of Magnetite Multilayers on Polymer Latex Microspheres. *Adv Mater* **1999**, *11*, 950-953.

(38) Caruso, F.; Spasova, M.; Susha, A.; Giersig, M.; Caruso, R. A. Magnetic Nanocomposite Particles and Hollow Spheres Constructed by a Sequential Layering Approach. *Chemistry of Materials* **2001**, *13*, 109-116.

(39) Voigt, A.; Buske, N.; Sukhorukov, G. B.; Antipov, A. A.; Leporatti, S.; Lichtenfeld, H.; Bäumler, H.; Donath, E.; Möhwald, H. Novel Polyelectrolyte Multilayer Micro-and Nanocapsules as Magnetic Carriers. *J Magn Magn Mater* **2001**, *225*, 59-66.

(40) Nakamura, M.; Katagiri, K.; Koumoto, K. Preparation of Hybrid Hollow Capsules Formed with Fe 3 O 4 and Polyelectrolytes Via the Layer-by-Layer Assembly and the Aqueous Solution Process. *J. Colloid Interface Sci.* **2010**, *341*, 64-68.

(41) Szczepanowicz, K.; Warszynski, P. Magnetically Responsive Liquid Core Polyelectrolyte Nanocapsules. *J. Microencapsulation* **2015**, *32*, 123-128.

(42) Lukasiewicz, S.; Szczepanowicz, K. In Vitro Interaction of Polyelectrolyte Nanocapsules with Model Cells. *Langmuir* **2014**, *30*, 1100-1107.

(43) Lukasiewicz, S.; Szczepanowicz, K.; Blasiak, E.; Dziedzicka-Wasylewska, M. Biocompatible Polymeric Nanoparticles as Promising Candidates for Drug Delivery. *Langmuir* **2015**, *31*, 6415-6425.

(44) Sun, S.; Zeng, H.; Robinson, D. B.; Raoux, S.; Rice, P. M.; Wang, S. X.; Li, G. Monodisperse MFe2O4 (M= Fe, Co, Mn) Nanoparticles. *J. Am. Chem. Soc.* **2004**, *126*, 273-279.

(45) Coey, J. M. In *Magnetism and magnetic materials;* Cambridge University Press: 2010; .

(46) Gorin, D. A.; Portnov, S. A.; Inozemtseva, O. A.; Luklinska, Z.; Yashchenok, A. M.; Pavlov, A. M.; Skirtach, A. G.; Mohwald, H.; Sukhorukov, G. B. Magnetic/Gold Nanoparticle Functionalized Biocompatible Microcapsules with Sensitivity to Laser Irradiation. *Phys. Chem. Chem. Phys.* **2008**, *10*, 6899-6905.

(47) Scotti, A.; Liu, W.; Hyatt, J.; Herman, E.; Choi, H.; Kim, J.; Lyon, L.; Gasser, U.; Fernandez-Nieves, A. The CONTIN Algorithm and its Application to Determine the Size Distribution of Microgel Suspensions. *J. Chem. Phys.* **2015**, *142*, 234905.